

# RECENT PROGRESSES IN LATTICE BOLTZMANN SIMULATIONS OF FLOW AND MULTI-COMPONENT REACTIVE TRANSPORT IN POROUS MEDIA

QINJUN KANG<sup>1</sup>, PETER C. LICHTNER<sup>1</sup>, DONGXIAO ZHANG<sup>2</sup>

<sup>1</sup>Hydrology, Geochemistry and Geology Group, Los Alamos National Laboratory, Los Alamos, NM 87545, USA.

<sup>2</sup>Mewbourne School of Petroleum and Geological Engineering, University of Oklahoma, Norman, OK 73019, USA.

## ABSTRACT

In recent years, the Lattice Boltzmann (LB) method has become a powerful numerical tool for simulating complex fluid flows and modeling physics and chemistry in fluids. Derived from the continuum Boltzmann equation used in statistical mechanics, the LB method has the advantage of describing non-equilibrium dynamics, especially in fluid-flow applications involving interfacial dynamics and complex boundaries, without simplifying the physics. In addition, the parallel structure inherent in the LB method makes it extremely suitable for parallel computing. Because of these features, the LB method affords the most comprehensive pore-scale approach to systematically investigate fundamental issues involving flow and reactive transport in porous media. In this paper, the state of the art of this method is discussed. Specifically, a multi-component LB model for simulating reactive transport in porous media at the pore scale is presented. In the model, a set of distribution functions is introduced to simulate fluid flow and solute transport. The LB equation for flow recovers the correct pore-scale continuity and Navier-Stokes equations. The LB equations for solute transport are modified to recover advection-diffusion equations for total concentrations at the pore scale. The model takes into account advection, diffusion, homogeneous reactions among multiple aqueous species, heterogeneous reactions between the aqueous solution and minerals, as well as changes in solid and pore geometry. Homogeneous reactions are described through local equilibrium mass action relations. Mineral reactions are treated kinetically through boundary conditions at the mineral surface. Simulation examples presented include crystal formation from a supersaturated solution without flow, hydrate formation during carbon dioxide sequestration in oceanic sediments, and injection of carbon dioxide saturated brine into a limestone rock with pore geometry derived from a thin section.

## 1. INTRODUCTION

A better understanding of multi-component flow and reaction in natural and man-made porous media is critical to a wide range of fields, including hydrology (groundwater quality), fossil energy (oil, gas, coalbed methane, clathrates), economic geology (mineral processing and development), geologic carbon sequestration (hydrodynamic and mineral

trapping of carbon), and materials manufacturing and degradation (polymer composites, concrete, building materials). This problem is notoriously difficult because it usually involves multiple scales (microscopic, macroscopic, and field) and multiple processes (advection, diffusion, and chemical reaction). The problem is further complicated by the evolution of the pore geometry due to chemical reactions, which may significantly and continuously modify the hydrologic properties of the medium. Changes in medium properties (e.g., porosity, fracture aperture, tortuosity, and mineral composition) result in changes in hydrologic properties such as permeability, effective mass diffusivity, mineral surface area, and local reaction rates. Therefore, these changes in medium properties (and hence in hydrologic properties) are coupled with fluid flow, solute transport, and reactions.

Fast reaction rates causing local concentration gradients and different transport regimes related to dead end and connected pores are strongly dependent upon pore-scale heterogeneity, which is lost at the continuum scale. Therefore, to quantitatively investigate their influence, it is necessary to account for advection-diffusion-reaction processes at the pore scale. Because of its importance, the problem of reactive transport at the pore scale has been studied extensively by various approaches, including semi-analytical, experimental, numerical, and a combination of these approaches under different simplifying assumptions [Daccord, 1987; Hoefner and Fogler, 1988; Wells et al., 1991; Janecky et al., 1992; Salles et al., 1993; Kelemen et al., 1995; Bekri et al., 1995, 1997; Fredd and Fogler, 1998; Dijk and Berkowiz, 1998; Kang et al., 2002, 2003, 2004, 2005, 2006].

Most numerical studies at the pore scale are for systems of one- or two- aqueous species, which significantly limits their applicability to real systems. In this study, we present a multi-component pore-scale model based on the LB method for simulating reactive transport in porous media for both homogeneous and heterogeneous reactions.

The LB method is a relatively new numerical method in computational fluid dynamics [e.g., Chen and Doolen, 1998]. It originated from lattice gas (LG) automata, a discrete particle kinetics approach utilizing a discrete lattice and discrete time. The LB equation can also be obtained from the Boltzmann equation used in statistical mechanics. Using a multi-scale expansion technique, one can prove that the LB equation for flow recovers the pore-scale Navier-Stokes equations in the nearly incompressible limit with an equation of state representing an ideal gas law, and the LB equation for transport recovers the pore-scale advection-diffusion-reaction equations. The LB method has the advantage of describing non-equilibrium dynamics, especially in fluid-flow applications involving interfacial dynamics and complex boundaries [Chen and Doolen, 1998]. In addition, because the LB algorithm is fully parallel, it is very efficient running on massively parallel computers. Since its appearance, it has been successfully applied to studies of a variety of flow and transport phenomena such as flow in porous media, turbulence, micro-flows, multiphase and multi-component flows, particulate suspensions, heat transfer, and reaction-diffusion.

In a previous study, Kang et al. [2002] developed a LB model to simulate coupled flow and chemical dissolution for a system of two aqueous species (one for reactant and the other for product) in porous media. They took a systematic approach in considering the dynamic processes of advection, diffusion, and reaction, as well as the complex geometry of natural porous media and its evolution caused by chemical reaction. The simulation

results agreed qualitatively with experimental and theoretical analyses conducted by other researchers.

Later on, Kang et al. [2003] extended this model so that it can simulate both dissolution and precipitation processes for single-aqueous-component systems. They simulated dissolution and precipitation of a single solute in a simplified porous medium, and studied the effects of Peclet and Damkohler numbers on solid alteration and solute concentration. They also investigated the conditions at which the effects of dissolution and precipitation on solid alteration can be reversed approximately and minimize hysteresis.

Recently, we generalized these models and developed a LB pore-scale model for simulating reactive transport in systems with multiple aqueous components and minerals [Kang et al., 2006]. This model takes into account advection, diffusion, homogeneous reactions among multiple aqueous species, heterogeneous reactions between the aqueous solution and minerals, as well as the resulting geometrical changes in pore space.

## 2. MODEL AND THEORY

In the LB method, the pore-scale flow of a single aqueous fluid phase can be simulated by the following evolution equation:

$$f_\alpha(\mathbf{x} + \mathbf{e}_\alpha \delta t, t + \delta t) = f_\alpha(\mathbf{x}, t) - \frac{f_\alpha(\mathbf{x}, t) - f_\alpha^{\text{eq}}(\rho, \mathbf{u})}{\tau}, \quad (1)$$

where  $f_\alpha$  is the particle-velocity-distribution function along the  $\alpha$  direction,  $\delta t$  is the time increment,  $\tau$  is the dimensionless relaxation time related to the kinematic viscosity by  $\nu = (\tau - 0.5)RT\delta t$  (with  $R$  the ideal gas constant and  $T$  the temperature of the fluid),  $\mathbf{e}_\alpha$  are the discrete velocities, and  $f_\alpha^{\text{eq}}$  is the corresponding equilibrium distribution function. If both  $\mathbf{e}_\alpha$  and  $f_\alpha^{\text{eq}}$  are appropriately chosen, equation (1) can be proved to recover the correct continuity and momentum equations at the Navier-Stokes level [Qian et al, 1992; Chen et al, 1992]:

$$\frac{\partial \rho}{\partial t} + \nabla \cdot (\rho \mathbf{u}) = 0, \quad (2)$$

$$\frac{\partial(\rho \mathbf{u})}{\partial t} + \nabla \cdot (\rho \mathbf{u} \mathbf{u}) = -\nabla p + \nabla \cdot [\rho \nu (\nabla \mathbf{u} + (\nabla \mathbf{u})^\top)], \quad (3)$$

where  $p = \rho RT$  is the fluid pressure. The fluid density and velocity are calculated using

$$\rho = \sum_\alpha f_\alpha, \quad (4)$$

$$\rho \mathbf{u} = \sum_\alpha \mathbf{e}_\alpha f_\alpha. \quad (5)$$

If we assume that the concentrations of the aqueous species are sufficiently low so that their effect on the density and velocity of the solution is negligible, then we can describe the reactive transport of solute species using another set of distribution functions,  $G_{\alpha j}$ , which satisfies a similar evolution equation as  $f_i$ :

$$G_{\alpha j}(\mathbf{x} + \mathbf{e}_\alpha \delta t, t + \delta t) = G_{\alpha j}(\mathbf{x}, t) - \frac{G_{\alpha j}(\mathbf{x}, t) - G_{\alpha j}^{\text{eq}}(\Psi_j, \mathbf{u})}{\tau_{\text{aq}}}, \quad (j = 1, \dots, N_C), \quad (6)$$

where  $N_C$  is the number of primary species in the system and  $\tau_{\text{aq}}$  is the dimensionless relaxation time related to the diffusivity of aqueous species by  $D = (\tau_{\text{aq}} - 0.5)RT\delta t$ . The

above equation can be proved to recover the pore-scale advection-diffusion equation for  $\Psi_j$ , the total concentration of the  $j$ th primary species. This quantity is defined in terms of the distribution function by the following equation:

$$\Psi_j = \sum_{\alpha} G_{\alpha j}, \quad (7)$$

similar to the density in the flow equation and may be positive or negative depending on the selection of primary species [Lichtner, 1985, 1996]. Here we have assumed that the homogeneous reactions are in instantaneous equilibrium and that the following mass action equations hold:

$$C_i = (\gamma_i)^{-1} K_i \sum_{j=1}^{N_C} (\gamma_j C_j)^{\nu_{ji}}, \quad (8)$$

where  $C_j$  and  $C_i$  are the concentrations of the  $j$ th primary and  $i$ th secondary species, respectively,  $\nu_{ji}$  is the stoichiometric coefficient,  $K_i$  is the equilibrium constant of the  $i$ th homogeneous reaction, and  $\gamma_i$  is the activity of the  $i$ th secondary species. Therefore, by formulating a LB equation for total concentration  $\Psi_j$  and replacing the rates of homogeneous reactions with mass action equations, we reduce the number of unknowns and evolution equations significantly.

Mineral reactions are represented by boundary conditions at the solid-fluid interfaces for the total concentrations given by

$$D \frac{\partial \Psi_j}{\partial n} = \sum_{m=1}^{N_m} \nu_{jm} I_m^*, \quad (9)$$

where  $n$  is the direction normal to the interfaces pointing toward the fluid phase, and  $I_m^*$  the  $m$ th mineral reactions at the mineral interfaces.  $I_m^*$  is assumed to have the form derived from transition state theory:

$$I_m^* = -k_m (1 - K_m Q_m). \quad (10)$$

In the above equation,  $k_m$  and  $K_m$  are the reaction rate and equilibrium constants, respectively, and the ion activity product  $Q_m$  is defined by

$$Q_m = \prod_{j=1}^{N_C} (\gamma_j C_j)^{\nu_{jm}}. \quad (11)$$

The treatment of heterogeneous reactions through boundary conditions in the form of equations (9)-(11) has the advantage over the continuum formulation which does not resolve the pore scale in that diffusion of solute species to and from the mineral surface is accounted for in the current method but not in the continuum formulation. As a result, if  $Q_m$  becomes very large due to supersaturation, the reaction rate  $I_m^*$  in the continuum formulation becomes unreasonably large as there is no constraint mechanism. However, in the current formulation, the reaction rate is limited by diffusion and remains a realistic value.

## 3. SIMULATION RESULTS AND DISCUSSION

**3.1. Crystal growth from supersaturated solution without fluid flow.** The simulation geometry is a two-dimensional cell of size  $h \times h$ , where  $h$  equals 200 (in lattice units) in this study. Initially, the domain is filled with a supersaturated solution with a concentration  $C_0$ . At time zero, a stable nucleus is introduced at the center of the domain. Crystal begins to grow subsequently. Simple dimensional analysis suggests that there are two important dimensionless parameters, which control the processes. They are the relative concentration or saturation ( $\psi = C_0/C_s$ ) and Damkohler number ( $Da$ ). The  $Da$  number is defined as  $k_r h/D$  and describes the effect of reaction relative to that of diffusion.

Figure 1 shows crystal structures at different  $Da$  numbers and at 2000, 3000, and 4000 solid particles (crystal mass). The solute saturation is 1.2. As we can see from (a), the crystal is not compact. As the  $Da$  number decreases, the process becomes more and more surface reaction-controlled. Compared to the reaction, the mass transfer via diffusion is now fast. The solute can be easily transported from the bulk to the liquid-solid interface located at the center area of the domain. Therefore, the crystal growth is expected to be more compact, centered with the initial nucleus. This result is consistent with that of the multiparticle diffusion-limited aggregation (MPDLA) simulation of solidification structures of alloy melt, in which the morphology transforms from open cluster-type structures, via compact coral-type structures, to compact faceted structures as the process changes from diffusion-controlled to interface kinetics-controlled [Das and Mittemeijer, 2001]. In addition, the crystal shape in case (d) is a fairly round shape if we take into account the randomness introduced in the growth. This indicates that our model is free of lattice grid effects, which exist in other numerical simulations of crystal growth [Das and Mittemeijer, 2001; Xiao et al., 1988]. In their studies, the final crystal shape depends on the lattice used in the numerical simulation, even for the case of isotropic growth.

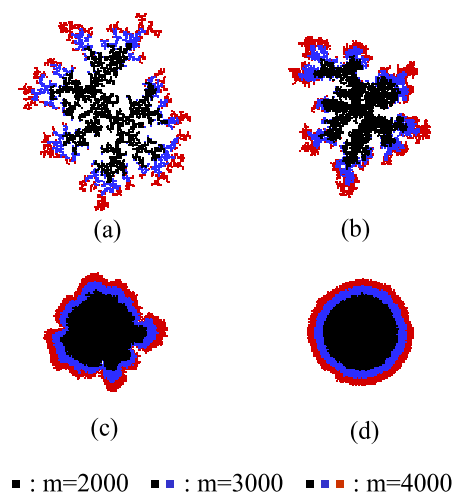


FIGURE 1. Crystal structures developed at different  $Da$  numbers and at solute saturation 1.2: (a)  $Da=600$ ; (b)  $Da=150$ ; (c)  $Da=48$ ; (d)  $Da=2$ .

**3.2. Hydrate formation during carbon dioxide sequestration in oceanic sediments.** Figure 2 shows the initial and final geometries due to hydrate formation during carbon dioxide sequestration in oceanic sediments at  $Pe = 62.8$  and different  $Da_{II}$  numbers. The Peclet number  $Pe$  and the second Damkohler number  $Da_{II}$  are defined as  $UL/D$  and  $k_r L/D$ , respectively, where  $U$  is the average steady-state velocity of the fluid over the entire domain,  $L$  is the length of the system in the transverse direction,  $D$  is the molecular diffusivity, and  $k_r$  is the reaction rate constant. Fluid flows from the top to the bottom. Regions in black correspond to the initial medium and regions in red depict hydrate formed. As  $Da_{II}$  decreases, the time (normalized by  $L^2/D$ ) needed to plug the medium increases. As shown in (a), hydrate formation mainly occurs at the upstream boundary for large  $Da_{II}$  numbers (fast kinetics), resulting in the quick blocking of the pore space and hence preventing the supersaturated solution from entering the medium. As the  $Da_{II}$  number decreases, the supersaturated solution penetrates further into the fractures and more hydrate is formed in the downstream part of the medium. There is no hydrate formed within the transverse channel connecting the two vertical fractures in case (a); some hydrate forms in case (b); and extensive hydrate formation occurs in case (c) and (d) that the fracture is plugged in both cases.

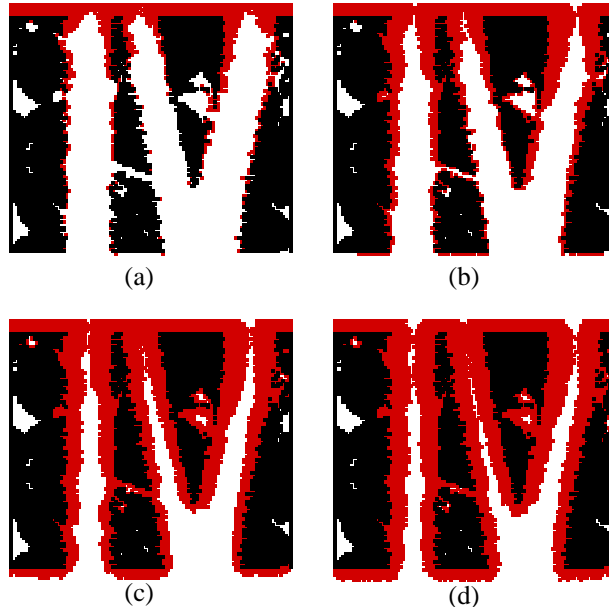


FIGURE 2. Initial and resulting geometries due to precipitation at  $Pe = 62.8$ : (a)  $Da_{II} = 32.4$ ,  $t^* = 0.0457$ ; (b)  $Da_{II} = 3.24$ ,  $t^* = 0.243$ ; (c)  $Da_{II} = 0.324$ ,  $t^* = 1.972$ ; (d)  $Da_{II} = 0.0324$ ,  $t^* = 17.118$ . Fluid flows from the top to the bottom. Regions in black correspond to the initial geometry and regions in red depict hydrate formed. Time  $t^*$  is normalized by  $L^2/D$ .

**3.3. Injection of carbon dioxide saturated brine into a limestone rock.** Pore scale calculations are carried out for injection of a fluid saturated with 170 bars  $\text{CO}_2(\text{g})$

into a limestone rock. Simulations are performed on a digitized image of a photographic image of the limestone rock thin section with  $640 \times 480$  pixels. Two different cases are considered with different mineral reaction rates to show their effects on solution concentration, mineral deposition and change in geometry. Calculations are performed for the chemical system:  $\text{Na}^+$ - $\text{Ca}^{2+}$ - $\text{Mg}^{2+}$ - $\text{H}^+$ - $\text{SO}_4^{2-}$ - $\text{Cl}^-$ - $\text{CO}_2$  with the reaction of calcite to form dolomite and gypsum. A constant pressure gradient is imposed across the domain. Secondary species included in the simulation are:  $\text{OH}^-$ ,  $\text{HSO}_4^-$ ,  $\text{H}_2\text{SO}_4(\text{aq})$ ,  $\text{CO}_3^{2-}$ ,  $\text{HCO}_3^-$ ,  $\text{CaCO}_3(\text{aq})$ ,  $\text{CaHCO}_3^+$ ,  $\text{CaOH}^+$ ,  $\text{CaSO}_4(\text{aq})$ ,  $\text{MgCO}_3(\text{aq})$ ,  $\text{MgHCO}_3^+$ ,  $\text{MgSO}_4(\text{aq})$ ,  $\text{MgOH}^+$ ,  $\text{NaCl}(\text{aq})$ ,  $\text{NaHCO}_3(\text{aq})$ ,  $\text{NaOH}(\text{aq})$ . Initial fluid composition is pH 7.75 and 2.69m NaCl brine, equilibrium with minerals calcite, dolomite and gypsum at  $25^\circ\text{C}$ . Initial rock composition is calcite. Secondary minerals include dolomite and gypsum. For boundary conditions, inlet fluid has pH 3.87 and is in equilibrium with 179 bars  $\text{CO}_2(\text{g})$  and minerals dolomite and gypsum. Zero gradient boundary conditions are imposed at the outlet. Resulting geometry, volume fraction of calcite, dolomite, and gypsum, concentration of total  $\text{Ca}^{2+}$ ,  $\text{Mg}^{2+}$ , and  $\text{SO}_4^{2-}$ , and pH at time=15625 s are plotted. Damkohler number is 7.375 for calcite and gypsum and 0.7375 for dolomite for the faster mineral reactions and  $7.375 \times 10^{-2}$  for calcite and gypsum and  $7.375 \times 10^{-3}$  for dolomite for slower reactions. Only resulting geometry is shown here (Figure 3) due to the limited space.

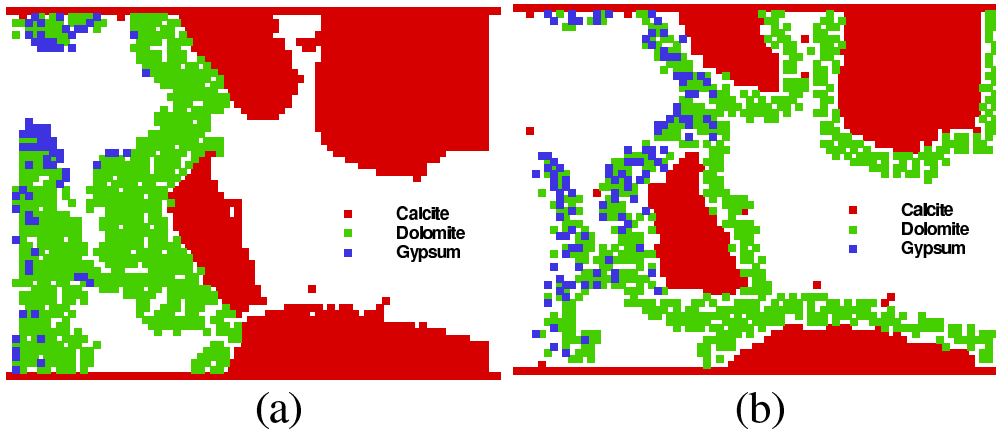


FIGURE 3. Resulting geometry for mineral reaction rate constants (a)  $10^{-6}$   $\text{mol}/\text{cm}^2/\text{s}$  for calcite and gypsum, and  $10^{-7}$   $\text{mol}/\text{cm}^2/\text{s}$  for dolomite; (b)  $10^{-8}$   $\text{mol}/\text{cm}^2/\text{s}$  for calcite and gypsum, and  $10^{-9}$   $\text{mol}/\text{cm}^2/\text{s}$  for dolomite.

As can be seen from the figures, as the reaction rate constants decrease, the deposition of dolomite becomes more uniform surrounding the dissolving calcite grains. Only a small amount of gypsum forms on top of dolomite. At some point in the simulation, the major pores for flow become blocked halting further fluid flow through the medium. The concentration of  $\text{CO}_2(\text{aq})$  and the pH are uniform over the entire pore space. For faster reactions, the reaction rates for all minerals are close to zero except in area close to entrance. For slower reactions, all reaction rates have finite values (negative for calcite and positive for dolomite and gypsum) at the mineral surface in the whole domain, outlining the solid geometry.

## REFERENCES

- Bekri et al., 1995. Bekri, S., J. F. Thovert, and P. M. Adler (1995), Dissolution of porous media, *Chem. Eng. Sci.*, *50*, 2765-2791.
- Bekri et al., 1997. Bekri, S., J. F. Thovert, and P. M. Adler (1997), Dissolution and deposition in fractures, *Eng. Geology*, *48*, 283-308.
- Chen and Doolen, 1998. Chen, S., and G.D. Doolen (1998), Lattice Boltzmann method for fluid flows, *Annu. Rev. Fluid Mech.*, *30*, 329-364.
- Chen et al., 1992. Chen, H., S. Chen, and W. H. Matthaeus (1992), Recovery of the Navier-Stokes equations using a lattice-gas Boltzmann method, *Phys. Rev. A.*, **45**, R5339-5342.
- Daccord, 1987. Daccord, G. (1987), Chemical dissolution of a porous medium by a reactive fluid, *Phys. Rev. Lett.*, *58*, 479-482.
- Das and Mittemeijer, 2001. Das, A. and E. J. Mittemeijer (2001), A Monte Carlo simulation of solidification structures of binary alloys, *Philo. Magaz. A*, *81*, 2725-2742.
- Dijk and Berkowiz, 1998. Dijk, P., and B. Berkowitz (1998), Precipitation and dissolution of reactive solutes in fracture, *Water Resour. Res.*, *34*, 457-470.
- Fredd and Fogler, 1998. Fredd, C. N., and H. S. Fogler (1998), Influence of transport and reaction on wormhole formation in porous media, *AIChE J.*, *44*, 1933-1949.
- Hoefner and Fogler, 1988. Hoefner, M. L., and H. S. Fogler (1988), Pore evolution and channel formation during flow and reaction in porous media, *AIChE J.*, *34*, 45-54.
- Janecky et al., 1992. Janecky, D. R., S. Chen, and S. Dawson, et al. (1992), Lattice gas automata for flow and transport in geochemical systems, In Proceeding, 7th Int. Symp. on Water-Rock Interaction. Y.K. Kharaka and A.S. Maest(Eds), A.A. Balkem a, Rotterdam, Netherlands, 1043.
- Kang et al., 2002. Kang, Q., D. Zhang, S. Chen, and X. He (2002), Lattice Boltzmann simulation of chemical dissolution in porous media, *Phys. Rev. E*, *65*, 036318.
- Kang et al., 2003. Kang, Q., D. Zhang, and S. Chen (2003), Simulation of dissolution and precipitation in porous media, *J. Geophys. Res.*, *108*, 2505.
- Kang et al., 2004. Kang, Q., D. Zhang, P. C. Lichtner, and I. N. Tsimpanogiannis (2004), Lattice Boltzmann model for crystal growth from supersaturated solution, *Geophys. Rev. Lett.*, *31*, L21604.
- Kang et al., 2005. Kang, Q., I. N. Tsimpanogiannis, D. Zhang, and P. C. Lichtner (2005), Numerical modeling of pore-scale phenomena during CO<sub>2</sub> sequestration in oceanic sediments, *Fuel Proce. Tech.*, *86*, 1647.
- Kang et al., 2006. Kang, Q., P. C. Lichtner and D. Zhang (2006), Lattice Boltzmann pore-scale model for multicomponent reactive transport in porous media, *J. Geophys. Res.*, in press.
- Kelemen et al., 1995. Kelemen, P. B., J. A. Whitehead, E. Aharonov, and K. A. Jordahl (1995), Experiments on flow focusing in soluble porous media, with applications to melt extraction from the mantle, *J. Geophys. Res.*, *100*, 475-496.
- Lichtner, 1985. Lichtner, P. C. (1985), Continuum model for simultaneous chemical reactions and mass transport in hydrothermal systems, *Geochimica et Cosmochimica ACTA*, *49*, 779-800.
- Lichtner, 1996. Lichtner, P. C. (1996), Continuum formulation of multicomponent-multiphase reactive transport, *Reviews in Mineralogy*, *34*, *Reactive Transport in Porous Media*, 1-81.
- Qian et al., 1992. Qian, Y., D. d'Humieres (1992), and P. Lallemand, Lattice BGK models for Navier-Stokes equation, *Europhys. Lett.*, **17**, 479-484.
- Salles et al., 1993. Salles, J., J. F. Thovert, and P. M. Adler (1993), Deposition in porous media and clogging, *Chem. Eng. Sci.*, *48*, 2839-2858.
- Wells et al., 1991. Wells, J. T., D. R. Janecky, and B. J. Travis (1991), A lattice gas automata model for heterogeneous chemical-reactions at mineral surfaces and in pore networks, *Physica D*, *47*, 115-123.
- Xiao et al., 1988. Xiao, R. F., J. I. D. Alexander, and F. Rosenberger (1988), Morphological evolution of growing crystals: A Monte Carlo simulation, *Phys. Rev. A* *38*, 2447-2455.